Lecture Notes on Graphene

W. Zhu[1]

[1] *Westlake Institute of Advanced Study,*

Westlake University, Hangzhou, P. C. China

Contents

Keywords: Crystal structure; Tight-binding Hamiltonian; Band structure; Symmetry; Dirac fermion

Carbon, is unique in that its electronic structure allows for hybridization to build up sp^3, sp^2, and sp networks and, hence, to form more known stable allotropes than any other element. The most common allotropic form of carbon is graphite which is an abundant natural mineral and together with diamond has been known since antiquity. The carbon atoms in the graphene layer form three σ bonds with neighboring carbon atoms by overlapping of sp^2 orbitals while the remaining p_z orbitals overlap to form a band of filled π orbitals – the valence band – and a band of empty π^* orbitals – the conduction band – which are responsible for the high in-plane conductivity.

For several decades the isolation of graphene monolayer seemed to be impossible on the basis of, among other things, theoretical studies on the thermodynamic stability of two-dimensional crystals. An important step in this direction was made by a research group in Manchester guided by Geim and Novoselov in 2004 who reported a method for the creation of single layer graphene on a silicon oxide substrate by peeling the graphite by micromechanical cleavage (scotch tape method). Graphene exhibited outstanding structural, electrical, and mechanical properties and six years later Novoselov and Geim were honored with the Nobel Prize in Physics "*for groundbreaking experiments regarding the two-dimensional material graphene.*"

TIGHT-BINDING MODEL

We will present the low-energy physics of graphene, two-dimensional honeycomb crystal with only one active orbital. The lattice vectors of honeycomb lattice are chosen as:

$$\mathbf{a}_1 = \frac{a}{2}(\sqrt{3}\hat{x} + 3\hat{y}), \mathbf{a}_2 = \frac{a}{2}(-\sqrt{3}\hat{x} + 3\hat{y}) \tag{1}$$

where a is the carbon-carbon distance between the same sublattice. The reciprocal-lattice vectors are given by

$$\mathbf{b}_1 = \frac{2\pi}{3a}(\sqrt{3}\hat{x} + \hat{y}), \mathbf{b}_2 = \frac{2\pi}{3a}(-\sqrt{3}\hat{x} + \hat{y}) \tag{2}$$

We choose the corner of Brillouim Zone (BZ) as $K = (-\frac{4\pi}{3a\sqrt{3}}, 0), K' = (\frac{4\pi}{3a\sqrt{3}}, 0)$.

The nearest-neighbor tight binding Hamiltonian:

$$H_0 = \sum_{i,\sigma} \varepsilon_{i,\sigma} a^\dagger_{i,\sigma} a_{i,\sigma} + \varepsilon_{i,\sigma} b^\dagger_{i,\sigma} b_{i,\sigma} + \sum_{\langle ij\rangle,\sigma} t_{ij}(a^\dagger_{i,\sigma} b_{j,\sigma} + h.c.) \tag{3}$$

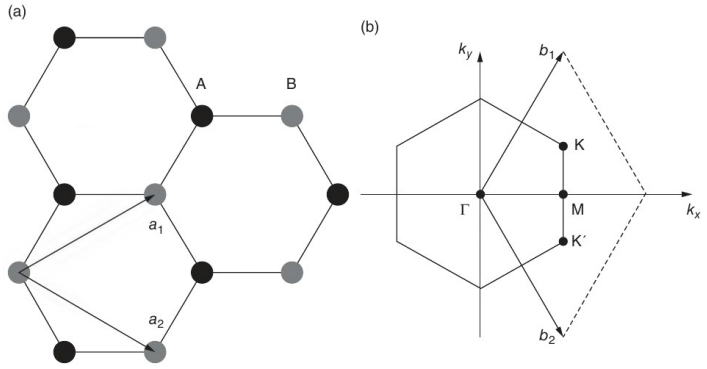

FIG. 1: Crystal structure of monolayer graphene.

where the sum is over pairs of nearest neighbors atoms i, j on the lattice. ε_i is the on-site energy which takes $\varepsilon_{A(B)}$ on A(B)-sublattice. $t_{ij} = t$ is the nearest-neighbor hopping energy. The Bloch trial wave function has to be built as a superposition of the atomic orbitals from the two atoms forming the primitive cell:

$$a^\dagger_{\mathbf{k},\sigma} = \frac{1}{\sqrt{N_A}} \sum_i e^{i\mathbf{k}\cdot\mathbf{r}_i} a^\dagger_{i,\sigma} \tag{4}$$

$$b^\dagger_{\mathbf{k},\sigma} = \frac{1}{\sqrt{N_B}} \sum_i e^{i\mathbf{k}\cdot\mathbf{r}_i} b^\dagger_{i,\sigma} \tag{5}$$

where $\mathbf{k}$ is the Bloch wave momentum. $N_A(B)$ is the number of A(B) atoms in the system.

After the Fourier transformation, we get the bloch Hamiltonian:

$$\hat{H}_0 = \sum_{\mathbf{k},\sigma} \left(a^\dagger_{\mathbf{k},\sigma}, b^\dagger_{\mathbf{k},\sigma}\right) \begin{pmatrix} H_{AA} & H_{AB} \\ H_{BA} & H_{BB} \end{pmatrix} \begin{pmatrix} a_{\mathbf{k},\sigma} \\ b_{\mathbf{k},\sigma} \end{pmatrix} = \sum_{\mathbf{k},\sigma} \left(a^\dagger_{\mathbf{k},\sigma}, b^\dagger_{\mathbf{k},\sigma}\right) [d_1\tau_x + d_2\tau_y + \varepsilon\tau_0 + \bar{\varepsilon}\tau_z] \begin{pmatrix} a_{\mathbf{k},\sigma} \\ b_{\mathbf{k},\sigma} \end{pmatrix} \tag{6}$$

where

$$H_{AA} = <\mathbf{k}A|H_0|\mathbf{k}A> = \frac{1}{N_A} \sum_{i,i'} e^{i\mathbf{k}(\mathbf{r}_{iA} - \mathbf{r}_{i'A})} < iA|H_0|i'A> = \varepsilon_A \tag{7}$$

$$H_{BB} = <\mathbf{k}B|H_0|\mathbf{k}B> = \frac{1}{N_B} \sum_{j,j'} e^{i\mathbf{k}(\mathbf{r}_{jA} - \mathbf{r}_{j'A})} < jB|H_0|j'B> = \varepsilon_B \tag{8}$$

$$\begin{aligned} H_{BA} &= <\mathbf{k}B|H_0|\mathbf{k}A> = \frac{1}{N_A} \sum_{i,j} e^{i\mathbf{k}\cdot(\mathbf{r}_{iA} - \mathbf{r}_{jB})} < jB|H_0|iA> = \frac{1}{N_A} \sum_{<ij>} e^{i\cdot k(\mathbf{r}_{iA} - r_{jB})} t_{ij} \\ &= t(e^{i\mathbf{k}\cdot\mathbf{a}_1} + e^{i\mathbf{k}\cdot\mathbf{a}_2} + e^{-i\mathbf{k}\cdot(\mathbf{a}_1+\mathbf{a}_2)}) = t(1 + 2\cos x \cos y) + it \sin x \cos y = d_1 + id_2 \\ H_{AB} &= H^*_{BA} \end{aligned} \tag{9}$$

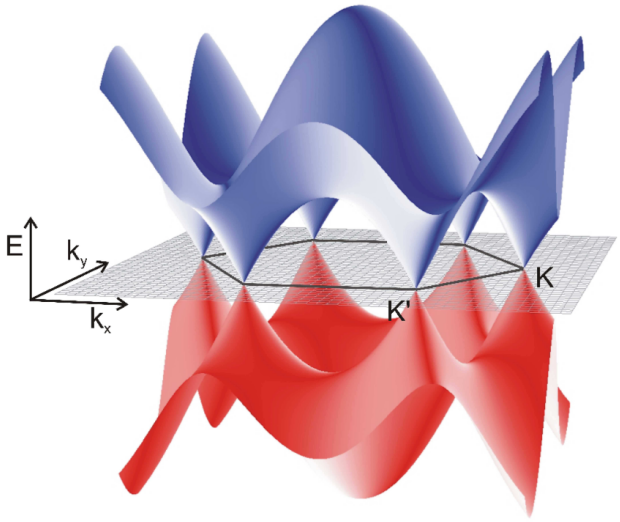

FIG. 2: Band structure of monolayer graphene.

where $x = k_x\sqrt{3}a/2$ and $y = k_y a/2$. Here we consider both sublattice A and B share the same corrdinates in real space.

Symmetry analysis

1. *Time-Reversal symmetry*

According to the definition, we know

$$\hat{T} = i\sigma_y K: \quad \hat{T} a^\dagger_{\mathbf{k},\sigma} \hat{T}^{-1} = (-\sigma) a^\dagger_{-\mathbf{k},-\sigma} \tag{10}$$

so we also know that

$$\hat{T}: \quad \hat{T} a^\dagger_{i,\sigma} \hat{T}^{-1} = (-\sigma) a^\dagger_{i,-\sigma} \tag{11}$$

since we have

$$\hat{T} a^\dagger_{i,\sigma} \hat{T}^{-1} = \hat{T} \sum_{\mathbf{k}} e^{i\mathbf{k}\cdot\mathbf{r}_i} \hat{T}^{-1} \hat{T} a^\dagger_{\mathbf{k},\sigma} \hat{T}^{-1} = \sum_{\mathbf{k}} e^{-i\mathbf{k}\cdot\mathbf{r}_i} (-\sigma) a^\dagger_{-\mathbf{k},-\sigma} = (-\sigma) a^\dagger_{i,-\sigma} \tag{12}$$

Then we can check the hamiltonian of both Eq. 3 and Eq. 6 are time-reversal invariant:

$$\begin{aligned}
\hat{T}\hat{H}_0\hat{T}^{-1} &= \hat{T}[\sum_{i,\sigma}\varepsilon_{i,\sigma}a^\dagger_{i,\sigma}a_{i,\sigma}+\varepsilon_{i,\sigma}b^\dagger_{i,\sigma}b_{i,\sigma}+\sum_{\langle ij\rangle,\sigma}t_{ij}(a^\dagger_{i,\sigma}b_{j,\sigma}+h.c.)]\hat{T}^{-1}\\
&= \sum_{i,\sigma}\varepsilon_{i,\sigma}\hat{T}a^\dagger_{i,\sigma}a_{i,\sigma}\hat{T}^{-1}+\varepsilon_{i,\sigma}\hat{T}b^\dagger_{i,\sigma}b_{i,\sigma}\hat{T}^{-1}+\sum_{\langle ij\rangle,\sigma}t^*_{ij}(\hat{T}a^\dagger_{i,\sigma}b_{j,\sigma}\hat{T}^{-1}+h.c.)\\
&= \sum_{i,\sigma}\varepsilon_{i,\sigma}(-\sigma)^2a^\dagger_{i,-\sigma}a_{i,-\sigma}+\varepsilon_{i,\sigma}(-\sigma)^2b^\dagger_{i,-\sigma}b_{i,-\sigma}+\sum_{\langle ij\rangle,\sigma}t^*_{ij}((-\sigma)^2a^\dagger_{i,-\sigma}b_{j,-\sigma}+h.c.)\\
&= \sum_{i,\sigma}\varepsilon_{i,\sigma}a^\dagger_{i,\sigma}a_{i,\sigma}+\varepsilon_{i,\sigma}b^\dagger_{i,\sigma}b_{i,\sigma}+\sum_{\langle ij\rangle,\sigma}t^*_{ij}(a^\dagger_{i,\sigma}b_{j,\sigma}+h.c.)=\hat{H}_0
\end{aligned}$$

, if the condition is satisfied: $t^*_{ij}=t_{ij}$.

$$\begin{aligned}
\hat{T}\hat{H}_0\hat{T}^{-1} &= \hat{T}[\sum_{\mathbf{k},\sigma}\left(a^\dagger_{\mathbf{k},\sigma},b^\dagger_{\mathbf{k},\sigma}\right)\begin{pmatrix}H_{AA}&H_{AB}\\H_{BA}&H_{BB}\end{pmatrix}\begin{pmatrix}a_{\mathbf{k},\sigma}\\b_{\mathbf{k},\sigma}\end{pmatrix}]\hat{T}^{-1}\\
&= [\sum_{\mathbf{k},\sigma}\left((-\sigma)a^\dagger_{-\mathbf{k},-\sigma},(-\sigma)b^\dagger_{-\mathbf{k},-\sigma}\right)\hat{T}\begin{pmatrix}H_{AA}&H_{AB}\\H_{BA}&H_{BB}\end{pmatrix}\hat{T}^{-1}\begin{pmatrix}(-\sigma)a_{-\mathbf{k},-\sigma}\\(-\sigma)b_{-\mathbf{k},-\sigma}\end{pmatrix}]\\
&= [\sum_{\mathbf{k},\sigma}\left((-\sigma)a^\dagger_{-\mathbf{k},-\sigma},(-\sigma)b^\dagger_{-\mathbf{k},-\sigma}\right)\begin{pmatrix}H^*_{AA}&H^*_{AB}\\H^*_{BA}&H^*_{BB}\end{pmatrix}\begin{pmatrix}(-\sigma)a_{-\mathbf{k},-\sigma}\\(-\sigma)b_{-\mathbf{k},-\sigma}\end{pmatrix}]\\
&= [\sum_{\mathbf{k},\sigma}\left((-\sigma)a^\dagger_{-\mathbf{k},-\sigma},(-\sigma)b^\dagger_{-\mathbf{k},-\sigma}\right)[d_1\tau_x-d_2\tau_y+\varepsilon\tau_0+\overline{\varepsilon}\tau_z]\begin{pmatrix}(-\sigma)a_{-\mathbf{k},-\sigma}\\(-\sigma)b_{-\mathbf{k},-\sigma}\end{pmatrix}]\\
&= [\sum_{\mathbf{k},\sigma}\left(a^\dagger_{-\mathbf{k},-\sigma},b^\dagger_{-\mathbf{k},-\sigma}\right)[d_1(-x,-y)\tau_x+d_2(-x,-y)\tau_y+\varepsilon\tau_0+\overline{\varepsilon}\tau_z]\begin{pmatrix}a_{-\mathbf{k},-\sigma}\\b_{-\mathbf{k},-\sigma}\end{pmatrix}]=\hat{H}_0
\end{aligned}$$

where T only has complex operation on matrix elements because the 2×2 matrix $H(\mathbf{k})=\begin{pmatrix}H_{AA}&H_{AB}\\H_{BA}&H_{BB}\end{pmatrix}$ is expressed in pseudospin space (by τ) not the spin space.

Please note that, under the time-reversal transformation, the total hamiltonian $\hat{H}_0$ is invariant, but the cornel $H(\mathbf{k})=\begin{pmatrix}H_{AA}&H_{AB}\\H_{BA}&H_{BB}\end{pmatrix}$ is NOT. Generally, the cornel hamiltonian is transferred like: $TH(\mathbf{k})T^{-1}=H(-\mathbf{k})$, which shows the momentum $\mathbf{k}$ is mapped to its time-reversal partner $-\mathbf{k}$. Here $H(\mathbf{k})$ and T are both matrix form, thus in many literatures people only discuss how the cornel hamiltonian $H(\mathbf{k})$ transforms instead of the whole hamiltonian operator $\hat{H}_0$!!

2. Inversion symmetry

According to the definition, we know

$$\hat{I}: \quad \hat{I}a^{\dagger}_{\mathbf{k},\sigma}\hat{I}^{-1} = b^{\dagger}_{-\mathbf{k},\sigma}, \quad \hat{I}b^{\dagger}_{\mathbf{k},\sigma}\hat{I}^{-1} = a^{\dagger}_{-\mathbf{k},\sigma} \tag{13}$$

so we also know that

$$\hat{I}: \quad \hat{I}a^{\dagger}_{i,\sigma}\hat{I}^{-1} = b^{\dagger}_{-i,\sigma}, \quad \hat{I}b^{\dagger}_{i,\sigma}\hat{I}^{-1} = a^{\dagger}_{-i,\sigma} \tag{14}$$

since we have

$$\hat{I}a^{\dagger}_{i,\sigma}\hat{I}^{-1} = \hat{I}\sum_{\mathbf{k}} e^{i\mathbf{k}\cdot\mathbf{r}_i}\hat{I}^{-1}\hat{I}a^{\dagger}_{\mathbf{k},\sigma}\hat{I}^{-1} = \sum_{\mathbf{k}} e^{i\mathbf{k}\cdot\mathbf{r}_i}b^{\dagger}_{-\mathbf{k},\sigma} = b^{\dagger}_{-i,\sigma} \tag{15}$$

Here we used the condition $\hat{I}\mathbf{r}\hat{I}^{-1} = -\mathbf{r}$ and $\hat{I}\mathbf{k}\hat{I}^{-1} = -\mathbf{k}$.

Then we can check the hamiltonian of both Eq. 3 and Eq. 6 are inversional invariant:

$$\begin{aligned}
\hat{I}\hat{H}_0\hat{I}^{-1} &= \hat{I}[\sum_{i,\sigma}\varepsilon_{i,\sigma}a^{\dagger}_{i,\sigma}a_{i,\sigma} + \varepsilon_{i,\sigma}b^{\dagger}_{i,\sigma}b_{i,\sigma} + \sum_{\langle ij\rangle,\sigma} t_{ij}(a^{\dagger}_{i,\sigma}b_{j,\sigma} + h.c.)]\hat{I}^{-1} \\
&= \sum_{i,\sigma}\varepsilon_{i,\sigma}\hat{I}a^{\dagger}_{i,\sigma}a_{i,\sigma}\hat{I}^{-1} + \varepsilon_{i,\sigma}\hat{I}b^{\dagger}_{i,\sigma}b_{i,\sigma}\hat{I}^{-1} + \sum_{\langle ij\rangle,\sigma} t_{ij}(\hat{I}a^{\dagger}_{i,\sigma}b_{j,\sigma}\hat{I}^{-1} + h.c.) \\
&= \sum_{i,\sigma}\varepsilon_{i,\sigma}b^{\dagger}_{-i,\sigma}b_{-i,\sigma} + \varepsilon_{i,\sigma}a^{\dagger}_{-i,\sigma}a_{-i,\sigma} + \sum_{\langle ij\rangle,\sigma} t_{ij}(b^{\dagger}_{-i,\sigma}a_{-j,\sigma} + h.c.) \\
&= \sum_{i,\sigma}\varepsilon_{-i,\sigma}b^{\dagger}_{i,\sigma}b_{i,\sigma} + \varepsilon_{-i,\sigma}a^{\dagger}_{i,\sigma}a_{i,\sigma} + \sum_{\langle ij\rangle,\sigma} t_{-i,-j}(b^{\dagger}_{i,\sigma}a_{j,\sigma} + h.c.) = \hat{H}_0
\end{aligned}$$

, if the conditions are satisfied: $\varepsilon_{-i,\sigma} = \varepsilon_{i,\sigma}$ and $t_{i,j} = t^{*}_{-j,-i}$.

In momentum space,

$$\begin{aligned}
\hat{I}\hat{H}_0\hat{I}^{-1} &= \hat{I}[\sum_{\mathbf{k},\sigma}\left(a^\dagger_{\mathbf{k},\sigma}, b^\dagger_{\mathbf{k},\sigma}\right)\begin{pmatrix} H_{AA} & H_{AB} \\ H_{BA} & H_{BB}\end{pmatrix}\begin{pmatrix} a_{\mathbf{k},\sigma} \\ b_{\mathbf{k},\sigma}\end{pmatrix}]\hat{I}^{-1} \\
&= [\sum_{\mathbf{k},\sigma}\left(b^\dagger_{-\mathbf{k},\sigma}, a^\dagger_{-\mathbf{k},\sigma}\right)\hat{I}\begin{pmatrix} H_{AA} & H_{AB} \\ H_{BA} & H_{BB}\end{pmatrix}\hat{I}^{-1}\begin{pmatrix} b_{-\mathbf{k},\sigma} \\ a_{-\mathbf{k},\sigma}\end{pmatrix}] \\
&= [\sum_{\mathbf{k},\sigma}\left(b^\dagger_{-\mathbf{k},\sigma}, a^\dagger_{-\mathbf{k},\sigma}\right)\begin{pmatrix} H_{AA}(\mathbf{k}) & H_{AB}(\mathbf{k}) \\ H_{BA}(\mathbf{k}) & H_{BB}(\mathbf{k})\end{pmatrix}\begin{pmatrix} b_{-\mathbf{k},\sigma} \\ a_{-\mathbf{k},\sigma}\end{pmatrix}] \\
&= [\sum_{\mathbf{k},\sigma}\left(b^\dagger_{-\mathbf{k},\sigma}, a^\dagger_{-\mathbf{k},\sigma}\right)[d_1(\mathbf{k})\tau_x + d_2(\mathbf{k})\tau_y + \varepsilon\tau_0 + \overline{\varepsilon}\tau_z]\begin{pmatrix} b_{-\mathbf{k},\sigma} \\ a_{-\mathbf{k},\sigma}\end{pmatrix}] \\
&= [\sum_{\mathbf{k},\sigma}\left(b^\dagger_{\mathbf{k},\sigma}, a^\dagger_{\mathbf{k},\sigma}\right)[d_1(-\mathbf{k})\tau_x + d_2(-\mathbf{k})\tau_y + \varepsilon\tau_0 + \overline{\varepsilon}\tau_z]\begin{pmatrix} b_{\mathbf{k},\sigma} \\ a_{\mathbf{k},\sigma}\end{pmatrix}] \\
&= [\sum_{\mathbf{k},\sigma}\left(a^\dagger_{\mathbf{k},\sigma}, b^\dagger_{\mathbf{k},\sigma}\right)[d_1(\mathbf{k})\tau_x + d_2(\mathbf{k})\tau_y + \varepsilon\tau_0 - \overline{\varepsilon}\tau_z]\begin{pmatrix} a_{\mathbf{k},\sigma} \\ b_{\mathbf{k},\sigma}\end{pmatrix}] \\
&= \hat{H}_0
\end{aligned}$$

, if and only if $\overline{\varepsilon} = 0$!! Please note that I doesnot change matrix elements because we put all operations on operators. Here we used the the quantity $d_1(-x,-y) = d_1(x,y)$ and $d_2(-x,-y) = -d_2(x,y)$.

An alternative way is,

$$\begin{aligned}
\hat{I}\hat{H}_0\hat{I}^{-1} &= \hat{I}[\sum_{\mathbf{k},\sigma}\left(a^\dagger_{\mathbf{k},\sigma}, b^\dagger_{\mathbf{k},\sigma}\right)\begin{pmatrix} H_{AA} & H_{AB} \\ H_{BA} & H_{BB}\end{pmatrix}\begin{pmatrix} a_{\mathbf{k},\sigma} \\ b_{\mathbf{k},\sigma}\end{pmatrix}]\hat{I}^{-1} \\
&= [\sum_{\mathbf{k},\sigma}\left(a^\dagger_{\mathbf{k},\sigma}, b^\dagger_{\mathbf{k},\sigma}\right)\hat{I}\begin{pmatrix} H_{AA} & H_{AB} \\ H_{BA} & H_{BB}\end{pmatrix}\hat{I}^{-1}\begin{pmatrix} a_{\mathbf{k},\sigma} \\ b_{\mathbf{k},\sigma}\end{pmatrix}] \\
&= [\sum_{\mathbf{k},\sigma}\left(a^\dagger_{\mathbf{k},\sigma}, b^\dagger_{\mathbf{k},\sigma}\right)\tau_x[d_1(-\mathbf{k})\tau_x + d_2(-\mathbf{k})\tau_y + \varepsilon\tau_0 + \overline{\varepsilon}\tau_z]\tau_x\begin{pmatrix} a_{\mathbf{k},\sigma} \\ b_{\mathbf{k},\sigma}\end{pmatrix}] \\
&= [\sum_{\mathbf{k},\sigma}\left(a^\dagger_{\mathbf{k},\sigma}, b^\dagger_{\mathbf{k},\sigma}\right)[d_1(-\mathbf{k})\tau_x - d_2(-\mathbf{k})\tau_y + \varepsilon\tau_0 - \overline{\varepsilon}\tau_z]\begin{pmatrix} a_{\mathbf{k},\sigma} \\ b_{\mathbf{k},\sigma}\end{pmatrix}] \\
&= [\sum_{\mathbf{k},\sigma}\left(a^\dagger_{\mathbf{k},\sigma}, b^\dagger_{\mathbf{k},\sigma}\right)[d_1(\mathbf{k})\tau_x + d_2(\mathbf{k})\tau_y + \varepsilon\tau_0 - \overline{\varepsilon}\tau_z]\begin{pmatrix} a_{\mathbf{k},\sigma} \\ b_{\mathbf{k},\sigma}\end{pmatrix}] \\
&= \hat{H}_0
\end{aligned}$$

, where we put operation on the hamiltonian cornel, that is $I \begin{pmatrix} H_{AA}(\mathbf{k}) & H_{AB}(\mathbf{k}) \\ H_{BA}(\mathbf{k}) & H_{BB}(\mathbf{k}) \end{pmatrix} \hat{I}^{-1} = \tau_x \begin{pmatrix} H_{AA}(-\mathbf{k}) & H_{AB}(-\mathbf{k}) \\ H_{BA}(-\mathbf{k}) & H_{BB}(-\mathbf{k}) \end{pmatrix} \tau_x$. The operation of $I = \tau_x \overline{K}$, where τ_x exchanges sublattice and $\overline{K}$ inverse momentum $\mathbf{k}$ to $-\mathbf{k}$.

3. Low-energy physics: Dirac fermion

Undoped graphene has a Fermi energy coinciding with the energy at the conical points, with a completely filled valence band, an empty conduction band, and no band gap in between. This means that, from the point of view of a general band theory, graphene is an example of a gapless semiconductor. Using the effective mass approximation, or $k \cdot p$ perturbation, the hamiltonian can be modeled by a chiral Dirac Hamiltonian, describes a linear relation between energy and momentum.

Around the momentum point **K**,

$$\begin{aligned} H_{BA} &= < kB|H_0|kA > \\ &= \frac{1}{N_A}\sum_{i,j} e^{i\vec{k}(r_{iA}-r_{jB})} < jB|H_0|iA > = \frac{1}{N}\sum_{<ij>} e^{i\vec{k}(r_{iA}-r_{jB})} t_{ij} \\ &= t(e^{ik_y a} + e^{i[-\frac{\sqrt{3}a}{2}(-\frac{4\pi}{3a\sqrt{3}}+k_x)-\frac{a}{2}k_y]} + e^{i[\frac{\sqrt{3}a}{2}(-\frac{4\pi}{3a\sqrt{3}}+k_x)-\frac{a}{2}k_y]}) = \mu \\ &\simeq t[(1+ik_y a) + 2(\cos\frac{2\pi}{3}\cos\frac{\sqrt{3}k_x a}{2} + \sin\frac{2\pi}{3}\sin\frac{\sqrt{3}k_x a}{2})(1 - i\frac{k_y a}{2})] \\ &= t[(1+ik_y a) + (-1+\frac{3ak_x}{2})(1-i\frac{k_y a}{2})] = \frac{3ta}{2}k_x + i\frac{3ta}{2}k_y \\ H_{AB} &= \mu^* \simeq \frac{3ta}{2}k_x - i\frac{3ta}{2}k_y \end{aligned} \tag{16}$$

Similarly, around another momentum point **K'**:

$$\begin{aligned}
H_{BA} &= < kB|H_0|kA > \\
&= \frac{1}{N_A}\sum_{i,j} e^{i\vec{k}(r_{iA}-r_{jB})} < jB|H_0|iA >= \frac{1}{N}\sum_{<ij>} e^{i\vec{k}(r_{iA}-r_{jB})}t_{ij} \\
&= t(e^{ik_y a} + e^{i[-\frac{\sqrt{3}a}{2}(\frac{4\pi}{3a\sqrt{3}}+k_x)-\frac{a}{2}k_y]} + e^{i[\frac{\sqrt{3}a}{2}(\frac{4\pi}{3a\sqrt{3}}+k_x)-\frac{a}{2}k_y]}) \\
&= t(e^{ik_y a} + 2\cos(\frac{2\pi}{3}+\frac{\sqrt{3}}{2}k_x a)e^{-i\frac{k_y a}{2}}) = \mu' \\
&\simeq t[(1+ik_y a) + 2(\cos\frac{2\pi}{3}\cos\frac{\sqrt{3}k_x a}{2} - \sin\frac{2\pi}{3}\sin\frac{\sqrt{3}k_x a}{2})(1-i\frac{k_y a}{2})] \\
&= t[(1+ik_y a) + (-1-\frac{3ak_x}{2})(1-i\frac{k_y a}{2})] = -\frac{3ta}{2}k_x + i\frac{3ta}{2}k_y \\
H_{AB} &= \mu^* \simeq -\frac{3ta}{2}k_x - i\frac{3ta}{2}k_y
\end{aligned} \tag{17}$$

The effective hamiltonian around K point is

$$\begin{aligned}
H_0 &= \begin{pmatrix} \varepsilon_A & \mu^* \\ \mu & \varepsilon_B \end{pmatrix} = \begin{pmatrix} \varepsilon_A & \frac{3ta}{2}k_x - i\frac{3ta}{2}k_y \\ \frac{3ta}{2}k_x + i\frac{3ta}{2}k_y & \varepsilon_B \end{pmatrix} \\
&= \hbar v_F \sigma\cdot\mathbf{k} + \sigma_0(\frac{\varepsilon_A+\varepsilon_B}{2}) + \sigma_z(\frac{\varepsilon_A-\varepsilon_B}{2})
\end{aligned} \tag{18}$$

where $\hbar v_F = 3ta/2$ is Fermi velocity ($v_f \approx 10^6 ms^{-1}$), $\boldsymbol{\sigma} = (\sigma_x, \sigma_y)$ are the Pauli matrices, $\boldsymbol{k} = (k_x, k_y)$ is a two-component particle momentum. Around **K'** point

$$\begin{aligned}
H_0 &= \begin{pmatrix} \varepsilon_A & \mu'^* \\ \mu' & \varepsilon_B \end{pmatrix} = \begin{pmatrix} \varepsilon_A & -\frac{3ta}{2}k_x - i\frac{3ta}{2}k_y \\ -\frac{3ta}{2}k_x + i\frac{3ta}{2}k_y & \varepsilon_B \end{pmatrix} \\
&= -\hbar v_F \sigma_x\cdot\mathbf{k_x} + \hbar v_F \sigma_y\cdot\mathbf{k_y} + \sigma_0(\frac{\varepsilon_A+\varepsilon_B}{2}) + \sigma_z(\frac{\varepsilon_A-\varepsilon_B}{2})
\end{aligned} \tag{19}$$

These equations are the Dirac equation. For undoped graphene, we set $\varepsilon_A = \varepsilon_B = 0$, and get gapless Dirac equation. In addition, we can adjust the sequence of basis$\{|KA>, |KB>, |K'B>, |K'A>\}$, and the Hamiltonian becomes

$$H_0 = \hbar v_F \tau_3 \otimes \sigma\cdot\mathbf{k} \tag{20}$$

where τ_3 applies to the valley space, $\sigma = \{\sigma_1, \sigma_2\}$ applies $A-B$ sublattice. $\otimes$ means that direct product,

$$\tau_3 \otimes \sigma_1 = \begin{pmatrix} 1 & 0 \\ 0 & -1 \end{pmatrix} \otimes \begin{pmatrix} 0 & 1 \\ 1 & 0 \end{pmatrix} = \begin{pmatrix} 0 & 1 & 0 & 0 \\ 1 & 0 & 0 & 0 \\ 0 & 0 & 0 & -1 \\ 0 & 0 & -1 & 0 \end{pmatrix}$$

Eigenstate and Eigenenergy For the Dirac equation,

$$H = \hbar v_f \boldsymbol{\sigma} \cdot \boldsymbol{k} = \hbar v_f \begin{pmatrix} 0 & k_x - ik_y \\ k_x + ik_y & 0 \end{pmatrix} = \hbar v_f k \begin{pmatrix} 0 & e^{-i\theta_{\boldsymbol{k}}} \\ e^{i\theta_{\boldsymbol{k}}} & 0 \end{pmatrix}, \tag{21}$$

where and $\theta_{\boldsymbol{k}} = \arctan(k_y/k_x)$ is the angle of momentum $\boldsymbol{k}$ down from the positive x-axis. The eigenvalues and corresponding eigenstates of (21) are

$$E_{\boldsymbol{k}\pm} = \pm \hbar v_f k \tag{22}$$

$$\Psi_{\boldsymbol{k}s}(\boldsymbol{r}) = \langle \boldsymbol{r} | \boldsymbol{k} s \rangle = \frac{e^{i\boldsymbol{k}\cdot\boldsymbol{r}}}{\sqrt{2A}} \begin{pmatrix} 1 \\ s e^{i\theta_{\boldsymbol{k}}} \end{pmatrix} \tag{23}$$

where $s = \pm$ denotes the chiral and A is the area of sample.

Transformation matrix The matrix $U_{\boldsymbol{k}}$ which implements the rotation from pseudospin to eigenstates basis has the form

$$\begin{aligned} U_{\boldsymbol{k}} = |\boldsymbol{k}+\rangle\langle \boldsymbol{k}\uparrow| + |\boldsymbol{k}-\rangle\langle \boldsymbol{k}\downarrow| =& \frac{1}{\sqrt{2}} \begin{pmatrix} 1 \\ e^{i\theta_k} \end{pmatrix} \begin{pmatrix} 1 & 0 \end{pmatrix} + \frac{1}{\sqrt{2}} \begin{pmatrix} 1 \\ -e^{i\theta_k} \end{pmatrix} \begin{pmatrix} 0 & 1 \end{pmatrix} \\ =& \frac{1}{\sqrt{2}} \begin{pmatrix} 1 & 1 \\ e^{i\theta_{\boldsymbol{k}}} & -e^{i\theta_{\boldsymbol{k}}} \end{pmatrix} \end{aligned} \tag{24}$$

Using $U_{\boldsymbol{k}}$, we can diagonal the Hamiltonian as

$$\begin{aligned} U_{\boldsymbol{k}}^\dagger H U_{\boldsymbol{k}} =& \frac{\hbar v_f k}{2} \begin{pmatrix} 1 & e^{-i\theta_{\boldsymbol{k}}} \\ 1 & -e^{-i\theta_{\boldsymbol{k}}} \end{pmatrix} \begin{pmatrix} 0 & e^{-i\theta_{\boldsymbol{k}}} \\ e^{i\theta_{\boldsymbol{k}}} & 0 \end{pmatrix} \begin{pmatrix} 1 & 1 \\ e^{i\theta_{\boldsymbol{k}}} & -e^{i\theta_{\boldsymbol{k}}} \end{pmatrix} \\ =& \hbar v_f k \begin{pmatrix} 1 & 0 \\ 0 & -1 \end{pmatrix} = \begin{pmatrix} E_{\boldsymbol{k}+} & 0 \\ 0 & E_{\boldsymbol{k}-} \end{pmatrix} \end{aligned} \tag{25}$$

Usually, we need to changing the electron momentum from one to another, for example $\boldsymbol{k}$ to $\boldsymbol{k}'$, it has to associate the spin rotation

$$U_{\boldsymbol{k}'}^\dagger U_{\boldsymbol{k}} = \frac{1}{2} \begin{pmatrix} 1 & e^{-i\theta_{\boldsymbol{k}'}} \\ 1 & -e^{-i\theta_{\boldsymbol{k}'}} \end{pmatrix} \begin{pmatrix} 1 & 1 \\ e^{i\theta_{\boldsymbol{k}}} & -e^{i\theta_{\boldsymbol{k}}} \end{pmatrix} = \frac{1}{2} \begin{pmatrix} 1 + e^{i\theta_{\boldsymbol{k}\boldsymbol{k}'}} & 1 - e^{i\theta_{\boldsymbol{k}\boldsymbol{k}'}} \\ 1 - e^{i\theta_{\boldsymbol{k}\boldsymbol{k}'}} & 1 + e^{i\theta_{\boldsymbol{k}\boldsymbol{k}'}} \end{pmatrix} \tag{26}$$

where $\theta_{\boldsymbol{k}\boldsymbol{k}'} = \theta_{\boldsymbol{k}} - \theta_{\boldsymbol{k}'}$.

Velocity The velocity in pseudospin basis is

$$v_x^s(\boldsymbol{k}) = \frac{\partial H}{\partial \hbar k_x} = v_f \sigma_x \tag{27}$$

$$v_y^s(\boldsymbol{k}) = \frac{\partial H}{\partial \hbar k_y} = v_f \sigma_y \tag{28}$$

Using transformation matrix $U_{\boldsymbol{k}}$, we can obtain velocity in eigen basis

$$v_x(\boldsymbol{k}) = U_{\boldsymbol{k}}^\dagger \frac{\partial H}{\partial \hbar k_x} U_{\boldsymbol{k}} = v_f(\cos\theta_{\boldsymbol{k}}\sigma_z + \sin\theta_{\boldsymbol{k}}\sigma_y) \tag{29}$$

$$v_y(\boldsymbol{k}) = U_{\boldsymbol{k}}^\dagger \frac{\partial H}{\partial \hbar k_y} U_{\boldsymbol{k}} = v_f(\sin\theta_{\boldsymbol{k}}\sigma_z - \cos\theta_{\boldsymbol{k}}\sigma_y) \tag{30}$$

This means that the electrons (holes) in graphene have a definite pseudospin direction, namely parallel (antiparallel) to the direction of motion. Thus, these states are chiral, as should be the case for massless Dirac fermions. This is of crucial importance for "relativistic" effects, such as Klein tunneling.

KLEIN PARADOX

After the discovery of the Dirac equation, Oskar Klein (1929) noticed one of its strange properties, which was called afterwards the "Klein paradox". Klein considered the 4×4 matrix Dirac equation for a relativistic spin-1/2 particle propagating in three-dimensional space. Soon after the discovery of graphene, it was realized that Klein tunneling (tunneling of Dirac fermions under the conditions of the Klein paradox) is one of the crucial phenomena for graphene physics and electronics (Katsnelson, Novoselov, and Geim, 2006). After the theoretical prediction of Klein tunneling in graphene, it was confirmed experimentally (Stander, Huard, and Goldhaber-Gordon, 2009; Young and Kim, 2009).

To be closer to our main subject, we will discuss the 2×2 matrix equation for a particle propagating in two-dimensional space; the essence of the paradox remains the same. We will consider the stationary Schrodinger equation

$$H \begin{pmatrix} \psi_1 \\ \psi_2 \end{pmatrix} = E \begin{pmatrix} \psi_1 \\ \psi_2 \end{pmatrix}, \tag{31}$$

$$H = -i\sigma\nabla + V(x, y) \tag{32}$$

where $V(x,y)$ is a potential energy. Let us consider the one-dimensional case $V = V(x)$ with a specific form of square potential

$$V(x) = \begin{cases} 0, x < -a \\ V_0, -a < x < a \\ 0, x > a \end{cases} \tag{33}$$

We consider electron propagation through the barrier for an arbitrary angle of incidence φ. The energy $E = \hbar v_F k$ is supposed to be positive. There is a refraction of the electron wave at the potential jump, and the new angle θ is determined by the conservation of the y-component of the electron momentum

$$k_y = k \sin\varphi = q_y = q \sin\theta \tag{34}$$

where

$$q = \frac{|E - V_0|}{\hbar v_F} \tag{35}$$

is the length of the wave vector within the barrier. For massless Dirac fermions with energy E propagating at the angle φ to the x-axis, the components of the spinor wave functions are related by (see Eq. 23)

$$\psi_2 = \psi_1 \exp(i\varphi) sgn(E) \tag{36}$$

Thus, the wave function has the following form

$$\psi_1(x,y) = \begin{cases} [e^{ik_x x} + re^{-ik_x x}]e^{ik_y y}, x < -a \\ [Ae^{iq_x x} + Be^{-iq_x x}]e^{ik_y y}, -a < x < a \\ te^{ik_x x}e^{ik_y y}, a < x \end{cases} \tag{37}$$

$$\psi_2(x,y) = \begin{cases} s[e^{ik_x x + i\varphi} - re^{-ik_x x - i\varphi}]e^{ik_y y}, x < -a \\ s'[Ae^{iq_x x + i\theta} - Be^{-iq_x x - i\theta}]e^{ik_y y}, -a < x < a \\ te^{ik_x x + i\varphi}e^{ik_y y}, a < x \end{cases} \tag{38}$$

where $s = sgn(E)$, $s' = sgn(E - V_0)$, $k_x = k\cos\varphi$, $q_x = q\cos\theta$. Here we have taken into account that the reflected particle moves at the angle $\pi - \varphi$, and $\exp[i(\pi - \varphi)] = -\exp(-i\varphi)$. The parameters r (the reflection coefficient), t (the transmission coefficient), A and B should

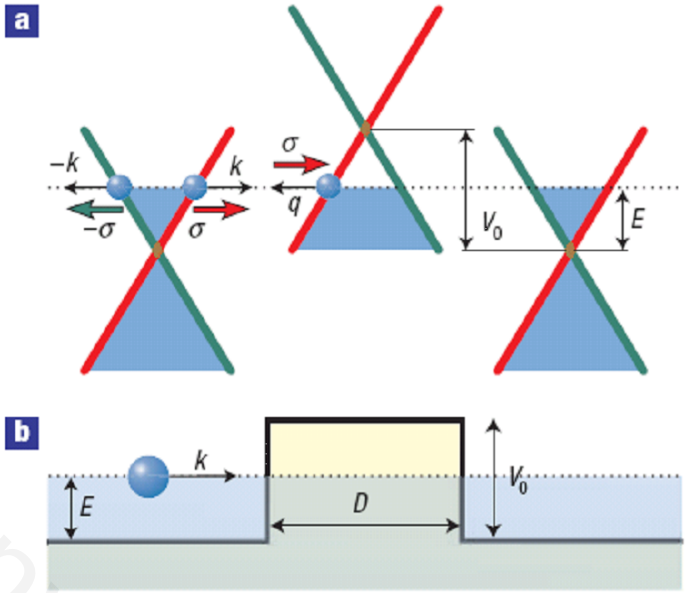

FIG. 3: Transformation of an electron to a hole under the potential barrier; the large arrows show directions of momenta, assuming that the group velocity is always parallel to the Ox axis. Black and gray lines show the dispersion of electronic states with opposite pseudospin projections.

be found from the continuity of ψ_1 and ψ_2 at $x = \pm a$. Note that the Klein paradox situation is $ss' = -1$, i.e. opposite signs of the energy outside and inside the barrier.

The continuum condition at $x = \pm a$ gives

$$[e^{-ik_x a} + re^{ik_x a}] = Ae^{-iq_x a} + Be^{iq_x a} \tag{39}$$

$$Ae^{iq_x a} + Be^{-iq_x a} = te^{ik_x a} \tag{40}$$

$$s[e^{-ik_x a + i\varphi} - re^{ik_x a - i\varphi}] = s'[Ae^{-iq_x a + i\theta} - Be^{iq_x a - i\theta}] \tag{41}$$

$$s'[Ae^{iq_x a + i\theta} - Be^{-iq_x a - i\theta}] = te^{ik_x a + i\varphi} \tag{42}$$

Solving these four equations leads to

$$r = 2e^{i\varphi - 2ik_x a} \sin(2q_x a) \frac{\sin\varphi - ss' \sin\theta}{ss'[e^{-2iq_x a}\cos(\varphi + \theta) + e^{2iq_x a}\cos(\varphi - \theta)] - 2i\sin(2q_x a)} \tag{43}$$

The transmission probability can be calculated as

$$T = |t|^2 = 1 - |r|^2. \tag{44}$$

The results are shown in Fig. 4. The most novel observation is $r = 0$ when $\varphi = 0$, i.e. the

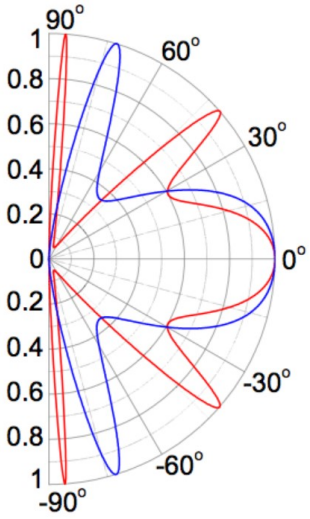

FIG. 4: Transmission probabilities through a 100-nm-wide barrier as a function of the angle of incidence for single-layer graphene. Fermi energies E of incident electrons 80 meV for single-layer. The barrier heights $V_0 = 200$ meV (blue curves) and (a) 285 meV (red curves).

electron wave full transmits without any influence by the potential barrier. This is quite different from the Schrodinger electron.

There are some other "full-transmission" angle for which $r = 0$, whatever the value of D, V_0 is. For example $\varphi = 0$ is such an angle. There are some other conditions, e.g.

$$\sin(2q_x a) = 0, or \;\; q_x a = \frac{\pi}{2} N. \tag{45}$$

Here, quantum tunneling in these materials becomes highly anisotropic, qualitatively different from the case of normal, nonrelativistic electrons.

This behavior is solely due to the negative energy solution in region II, and we can call it Klein tunneling since it has the same origin as Klein paradox. This is totally from the band structure of graphene.

VESELAGO LENSES

For massless particles with a linear dispersion, the group velocity is

$$\vec{v}_g = \pm v_F \frac{\vec{k}}{k}, \tag{46}$$

where the signs + and - correspond to electrons and holes, respectively. The incident electron wave has the wave vector $\vec{k} = k(\cos\varphi, \sin\varphi)$ and the group velocity $\vec{v}_e = v(\cos\varphi, \sin\varphi)$.

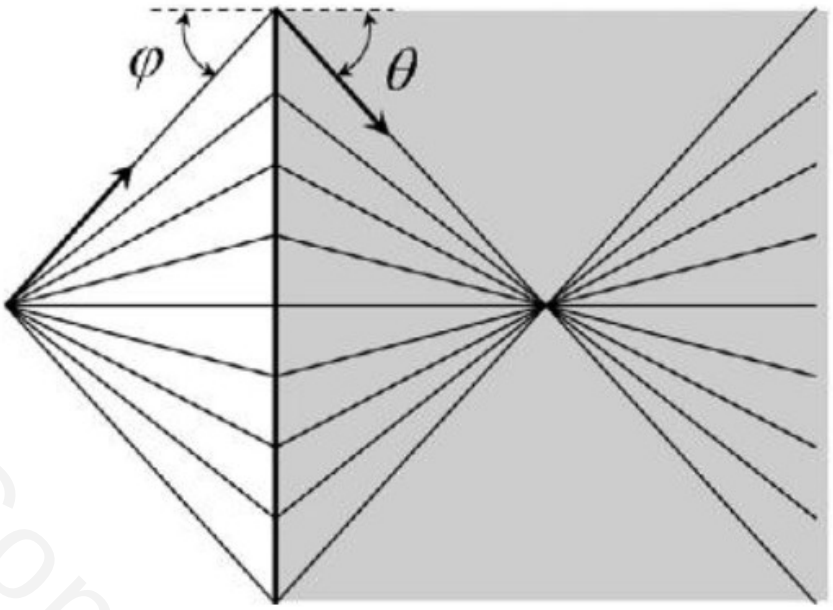

FIG. 5: A Veselago lens for the case of a negative refraction index. The refraction angle θ' is equal to $\theta' = -\theta$ in the plot.

The reflected wave has the wave vector $\vec{k}' = k(-\cos\varphi, \sin\varphi)$ and the group velocity $\vec{v}'_e = v(-\cos\varphi, \sin\varphi)$. For the transimitted wave, in the situation of the Klein paradox (or p-n junction), the group velocity is $\vec{v}_h = v(\cos\theta', \sin\theta')$, relating to the wave vector $\vec{q} = -q(\cos\theta', \sin\theta')$ with $\cos\theta' > 0$ and $q = \frac{|E-V_0|}{\hbar v_F}$. Please note that the refraction angle is $\theta' = -\theta$ in the plot. The refraction angle θ' is determined by the continuity of the y-component of the wave vector,

$$-q\sin\theta' = k\sin\varphi \Rightarrow n \equiv \frac{\sin\theta'}{\sin\varphi} = -\frac{k}{q} \tag{47}$$

with a negative refractive index n.

This means that the p-n junction in graphene transforms a divergent electron beam into a collimated one. This is because, in the p-n junction made of graphene, the group velocity $\vec{v}_g$ is parallel to the wave vector $\vec{k}$ for electrons and antiparallel for holes.

In optics, such devices are known as Veselago lenses (Veselago, 1968), and materials with negative refractive indices are called left-handed materials, or metamaterials (Pendry, 2004). Creation of such a material for visual light is not an easy task. For electrons in graphene such a situation can be realized quite easily.

Electron Veselago lensing in graphene was experimentally observed by Lee, Park, and

Lee (2015) and by Chen et al. (2016). Boggild et al. (2017) suggested a concept of "Dirac Fermion Microscope" where collimated electron beams in graphene in the ballistic regime are used to magnify atomic-scale inhomogeneities.

LANDAU LEVEL

Traditional two-dimensional electron gas

We start with traditional two-dimensional electron gas in the presence of strong magnetic field

$$H_0 = \frac{1}{2m}(\mathbf{p} - e\mathbf{A})^2 \tag{48}$$

where

$$\mathbf{p} = -i\hbar(\frac{\partial}{\partial x}, \frac{\partial}{\partial y}) \tag{49}$$

and magnetic field is $\mathbf{B} = \nabla \times \mathbf{A}$, gauge field is $\mathbf{A}$ as Landau gauge

$$\mathbf{A} = Bx\hat{e}_y \tag{50}$$

Since k_y is a good quantum number, we set $\psi(x, y) = e^{ik_y y}\phi(x)$,and

$$-\frac{\hbar^2}{2m}\phi''(x) + \frac{1}{2}m\omega_c^2(x - x_c)^2\phi(x) = E\phi(x) \tag{51}$$

where cycltron motion frequency $\omega_c = \frac{eB}{m}$, and cycltron center $x_c = -l_c^2 k_y$. $\phi(x)$ satisfies the same equation as one-dimensional simple harmonics. Thus we get the eigenvalue and eigenfunction

$$E_n = (n + \frac{1}{2})\hbar\omega_c = (n + \frac{1}{2})\hbar\frac{eB}{mc}, \quad n = 0, 1, 2... \tag{52}$$

$$\langle r|nk\rangle = \psi_{n,k_y}(x, y) = (\frac{1}{\pi l_c^2})^{\frac{1}{4}}\frac{1}{\sqrt{2^n n!}}e^{ik_y y}e^{-\frac{1}{2}\left(\frac{x+l_c^2 k_y}{l_c}\right)^2}H_n\left(\frac{x + l_c^2 k_y}{l_c}\right) \tag{53}$$

Here $n = 0, 1, 2...$ is non-negative integer,$l_c = \sqrt{\frac{\hbar}{eB}}$ is cycltron motion length. $H_n(x)$ is Hermit polynomial.

The eigenvalue is discrete, called Landau Level. For each Landau level, it is highly degenerated. In the Landau gauge, we denote

$$k_y = \frac{2\pi}{L_y}m, \quad m = 0, 1, 2, \cdots, N_\phi \tag{54}$$

The degenracy N_ϕ is determined by

$$0 \leq x_c \leq L_x \tag{55}$$

which leads to the condition

$$0 \leq l_c^2 k_y = \frac{\hbar}{eB}\frac{2\pi}{L_y} N_\phi \leq L_x \tag{56}$$

So we get

$$N_\phi = \frac{L_x L_y eB}{2\pi\hbar} = \frac{\Phi}{\phi_0} = \frac{L_x L_y}{2\pi l_c^2} \tag{57}$$

$\phi_0 = h/e$ is flux quanta. $\Phi = L_x L_y B$ is the total flux. The stronger magnetic field is, the larger degeneracy is.

FIG. 6: Landau level

Graphene

We write the Hamiltonian of graphene in the presence of magnetic field as

$$H = v_F\, \sigma \cdot (\mathbf{p} + e\mathbf{A}) \tag{58}$$

Pauli matrix is

$$\sigma = (\sigma_x, \sigma_y) \tag{59}$$

and vector potential is $\mathbf{A} = Bx\hat{e}_y$.

$$\begin{pmatrix} 0 & -iv_F[\hbar\frac{\partial}{\partial x} + (p_y + eBx)] \\ -iv_F[\hbar\frac{\partial}{\partial x} - (p_y + eBx)] & 0 \end{pmatrix} \begin{pmatrix} \psi_1 \\ \psi_2 \end{pmatrix} = E \begin{pmatrix} \psi_1 \\ \psi_2 \end{pmatrix}$$

equivalent to

$$\begin{cases} -iv_F[\hbar\frac{\partial}{\partial x} - (p_y + eBx)]\psi_1 = E\psi_2 \\ -iv_F[\hbar\frac{\partial}{\partial x} + (p_y + eBx)]\psi_2 = E\psi_1 \end{cases}$$

and

$$-v_F^2[\hbar\frac{\partial}{\partial x}+(\hbar k_y+eBx)][\hbar\frac{\partial}{\partial x}-(\hbar k_y+eBx)]\psi_1=E^2\psi_1 \tag{60}$$

and

$$\begin{aligned} v_F^2(-\hbar^2\partial_x^2+e^2B^2x^2+eB[\hbar\partial_x,x])\psi_1 &= E^2\psi_1 \\ (-\partial_x^2+\frac{1}{l_c^4}x^2+\frac{1}{l_c^2})\psi_1 &= \frac{E^2}{(\hbar v_F)^2}\psi_1 \end{aligned} \tag{61}$$

We see, it is actually a simple harmonic problem again.

We get eigenvalue

$$E_{n,s}=s\sqrt{2n}(eB\hbar^2v_F^2)^{1/2}=s\sqrt{2n}\hbar\omega_c, n=0,1,2...,s=\pm1 \tag{62}$$

where $l_c=\sqrt{\hbar/eB}$,$\omega_c=\frac{v_F}{l_c}$, $s=\pm$is for conduction and valence band.

Eigenvector of $n=0$ is special:

$$\langle r|0,k_y\rangle=\frac{e^{ik_yy}}{\sqrt{L_y}}\begin{pmatrix}0\\ \phi_{0,k_y}\end{pmatrix} \tag{63}$$

for other $n=1,2,3...$ are

$$\langle r|n,k_y\rangle=\frac{e^{ik_yy}}{\sqrt{2}\sqrt{L_y}}\begin{pmatrix}-is\phi_{n-1,k_y}\\ \phi_{n,k_y}\end{pmatrix} \tag{64}$$

We can combine them together in a compact form:

$$\langle r|n,k_y\rangle=\frac{\lambda}{\sqrt{L_y}}e^{ik_yy}\begin{pmatrix}-is\phi_{n-1,k_y}\\ \phi_{n,k_y}\end{pmatrix},\begin{cases}\lambda=1, & n=0\\ \lambda=\frac{1}{\sqrt{2}}, & n\neq0\end{cases} \tag{65}$$

$$\phi_{n,k_y}=(\frac{1}{\pi l_c^2})^{\frac{1}{4}}\frac{1}{\sqrt{2^nn!}}\exp^{-\frac{1}{2}\left(\frac{x+l_c^2k_y}{l_c}\right)^2}H_n\left(\frac{x+l_c^2k_y}{l_c}\right) \tag{66}$$

Degeneracy is, $k_y=2\pi m/L_y, m=0,1,\cdots,N_\phi$,

$$N_\phi=\frac{L_xL_yeB}{2\pi\hbar}=\frac{\Phi}{\phi_0} \tag{67}$$

This is for the K-point. For another K'-point, Hamiltonain is a 4×4 matrix

$$\hat{H}=\hbar v_F\begin{bmatrix}0 & \hat{k}_x-i(\hat{k}_y+\frac{x}{l_c^2}) & 0 & 0\\ \hat{k}_x+i(\hat{k}_y+\frac{x}{l_c^2}) & 0 & 0 & 0\\ 0 & 0 & 0 & -\hat{k}_x+i(\hat{k}_y+\frac{x}{l_c^2})\\ 0 & 0 & -\hat{k}_x-i(\hat{k}_y+\frac{x}{l_c^2}) & 0\end{bmatrix}. \tag{68}$$

The eigenvalue is

$$E = \mathrm{sgn}(n)\frac{\sqrt{2}v_F}{l_c}\sqrt{|n|} \tag{69}$$

Eigenstate is

$$\begin{bmatrix} F_A^K(\mathbf{r}) \\ F_B^K(\mathbf{r}) \end{bmatrix} = \frac{\lambda}{\sqrt{L_y}} e^{i\,k_y\,y} \begin{bmatrix} (-i)\mathrm{sgn}(n)\psi_{(|n|-1)}\left(x + l_c^2 k_y\right) \\ \psi_{(|n|)}\left(x + l_c^2 k_y\right) \end{bmatrix} \tag{70}$$

and

$$\begin{bmatrix} F_B^{K'}(\mathbf{r}) \\ F_A^{K'}(\mathbf{r}) \end{bmatrix} = \frac{\lambda}{\sqrt{L_y}} e^{i\,k_y\,y} \begin{bmatrix} (-i)\mathrm{sgn}(n)\psi_{(|n|-1)}\left(x + l_c^2 k_y\right) \\ \psi_{(|n|)}\left(x + l_c^2 k_y\right) \end{bmatrix}, \tag{71}$$

and

$$\begin{cases} \lambda = 1, \quad n = 0 \\ \lambda = \dfrac{1}{\sqrt{2}}, \quad n \neq 0 \end{cases} \tag{72}$$

$$\psi_{(|n|)}\left(x + l_c^2 k_y\right) = \left(\frac{1}{\pi l_c^2}\right)^{\frac{1}{4}} \frac{1}{\sqrt{2^{|n|}|n|!}} H_{|n|}\left(\frac{x + l_c^2 k_y}{l_c}\right) e^{-\frac{1}{2}\left(\frac{x + l_c^2 k_y}{l_c}\right)^2} \tag{73}$$

So we see, it forms the Landau level in graphene too. But, be different from the traditional electron gas, Landau level is not equally separated.

Moreover, $n = 0$ Landau level is special. Appearance of $E = 0$ Landau level is from the electron-hole symmetry. $n = 0$ eigenstate is localized on a single sublattice, i.e. A-site for K-point and B-site for K'-point. This is another interesting point.

BOUNDARY CONDITIONS AND NANORIBBONS

For the case of pure zigzag edges all missing atoms belong to sublattice A only (or sublattice B only), thus the corresponding components of the wave function for the two valleys, K and K', should vanish at the boundary. If we have a nanoribbon of a constant width L with zigzag edges, one edge corresponds to the missing atoms A and the other to the missing atoms B. The boundary conditions are

$$\psi_1(y = -L/2) = 0, \psi_2(y = L/2) = 0 \tag{74}$$

in the Dirac approximation we can consider them independently. For the valley K, the Schrodinger equation reads

$$(\partial_x + i\partial_y)\psi_1(x,y) = i(E/\hbar v_F)\psi_2 \tag{75}$$

$$(\partial_x - i\partial_y)\psi_2(x,y) = i(E/\hbar v_F)\psi_1 \tag{76}$$

Let us try the solutions as

$$\psi_1(x,y) = e^{ik_x x}u(y), \psi_2(x,y) = e^{ik_x x}v(y) \tag{77}$$

where u and v satisfy a system of two linear ordinary differential equations with constant coefficients ($k \equiv E/(\hbar v_F)$):

$$(k_x + \frac{d}{dy})u(y) = kv(y) \tag{78}$$

$$(k_x - \frac{d}{dy})v(y) = ku(y) \tag{79}$$

The ansatz solution could be

$$u(y) = Ae^{zy} + Be^{-zy} \tag{80}$$

$$v(y) = Ce^{zy} + De^{-zy} \tag{81}$$

with $z = \sqrt{k_x^2 - k^2}$. z can be either real (for evanescent waves) or imaginary (for propagating waves). On substituting this ansatz into Schrodinger equation and taking into account boundary condition ($u(L/2) = 0, v(-L/2) = 0$), one finds a dispersion relation for the waves in the nanoribbon:

$$\varphi(z) = \frac{k_x - z}{k_x + z} = e^{-2Lz} \tag{82}$$

The trivial solution $z = 0$ exists. The non-zero real z solution exists for $k_x L > 1$. The non-zero real z solution relates to the edge state, which lives close to the boundary with a decay decrement $z = k_x$ along the y-direction. This state are localized on the left and right edges of ribbon.

On the other hand, imaginary z also exists, relating to the standing wave which are bulk states.

The whole energy bands for the zigzag condition is shown in Fig. 7. The lowest band is the localied edge state.

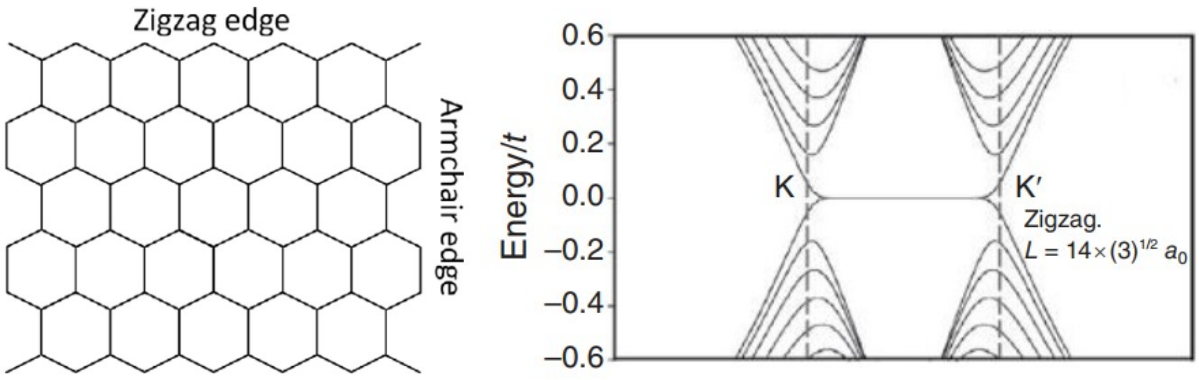

FIG. 7: The energy spectrum for zigzag-terminated graphene nanoribbon with 56 atoms per unit cell.

TWISTED GRAPHENE WITH MOIRE POTENTIALS

At last we discuss the electronic structure of twisted bilayer graphene. Essential simplifications happen for the case of a small misorientation angle θ in the continuum approximation, that is, for the electronic states in the vicinity of conical points K and K'. For small θ, intervalley scattering processes are negligible, and we can restrict ourselves to considering the vicinity of the K point only. The position of the K point in the second (rotated) layer is given by the vector

$$\vec{K}^{\theta} = R(\theta)\vec{K} = \vec{K} + \Delta\vec{K} \approx \vec{K} + \theta\vec{z} \times \vec{K} \tag{83}$$

where we only work in the small angle limit and take the first order in θ.

Then, without taking into account interlayer hopping, the Hamiltonian of two nonconnected graphene layers can be derived from Dirac equation by the corresponding changes of the coordinate system:

$$H_0 = \hbar v_F \sum_{\vec{k}} \psi^{\dagger}_{k+\Delta\vec{K}/2}\sigma \cdot (\vec{k} + \Delta\vec{K}/2)\psi_{k+\Delta\vec{K}/2} + \psi^{\dagger}_{k-\Delta\vec{K}/2}\sigma \cdot (\vec{k} - \Delta\vec{K}/2)\psi_{k-\Delta\vec{K}/2} \tag{84}$$

We now couple the Dirac points together by interlayer hopping terms :

$$H_{UD} = T_0(\mathbf{r})\sigma^0 + T_{AB}(\mathbf{r})\sigma^+ + T_{BA}(\mathbf{r})\sigma^- \tag{85}$$

Let us now derive the form of the tunneling matrix elements - for better intuition first consider very local tunneling (i.e. electrons tunnel only when the atoms of the two layers occlude each other). We then need to consider three cases, where (i) the atoms of both

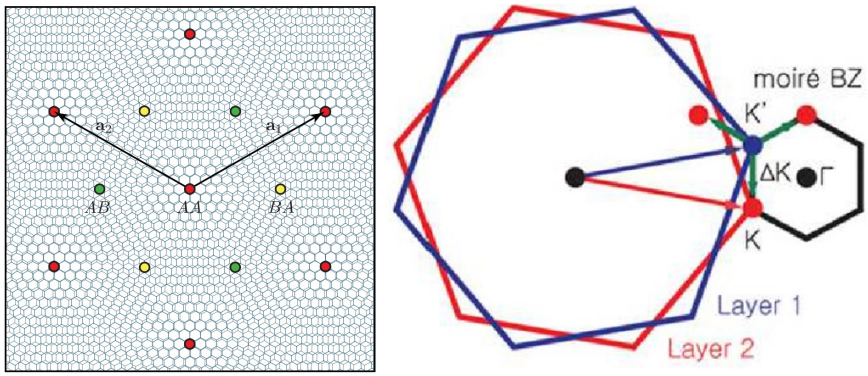

FIG. 8: (Left) Real space visualization of the moiré pattern and depiction of the AA stacking $r = 0$, AB stacking $r = -r_0$, and BA stacking $r = r_0$ points. All three of these points map to themselves up to shifts by lattice vectors under C_3 symmetry. (Right) Formation of moiré Brillouin zone. Red and blue hexagonal zones are original SLG's Brillouin zones from two layers, which are rotated clockwise and counterclockwise, respectively. ΔK is the momentum difference between two Dirac points, which can be controlled by the twist angle. Γ is the center of moiré Brillouin zone.

sublattices are on top of each other, the so called AA or equivalently the BB regions which form a triangular lattice, see Figure 1; (ii) where the A atoms of the lower layer align with the B atoms of the upper layer (AB regions), they form one sublattice of a honeycomb lattice on the moire scale; and finally (iii) the BA regions, where B atoms of the lower layer align with the A atoms of the upper layer and form the other sublattice of the honeycomb lattice on the moire scale.

Tunneling, say in the AA regions, could be represented as: $T_0 \sim \sum_n \delta(\mathbf{r} - \mathbf{R_n})$ where the sum runs over the triangular moire lattice sites locations. From the Poisson resummation formula this can be equivalently written as $\sum_n \delta(r - R_n) = A_M \sum_m \exp(-i\mathbf{G}_m \cdot \mathbf{r})$, where A_M is the area of the moire unit cell and $\mathbf{G}_m$ are the moire lattice reciprocal vectors. On the other hand the tunneling matrix elements in the other regions acquire additional phase factors due to their displacement from the unit cell centers. They are $T_{AB} \sim \sum_n \delta(\mathbf{r} - \mathbf{R}_n - \mathbf{r}_A) = A_M \sum_m e^{i\mathbf{G}_m \cdot \mathbf{r}_A} e^{-i\mathbf{G}_m \cdot \mathbf{r}}$ and $T_{BA} \sim \sum_n \delta(\mathbf{r} - \mathbf{R}_n - \mathbf{r}_B) = A_M \sum_m e^{i\mathbf{G}_m \cdot \mathbf{r}_B} e^{-i\mathbf{G}_m \cdot \mathbf{r}}$. In reality, one has to take into account a more general interlayer hopping $T(\mathbf{r})$ with Fourier components $T \sim (\mathbf{G}_m)$. Since the interlayer hopping depends on the 3D separation between atoms, and the separation between layers is more than twice the intralayer atomic separations, we expect the Fourier components to decrease rapidly and we can keep the lowest order harmonics.

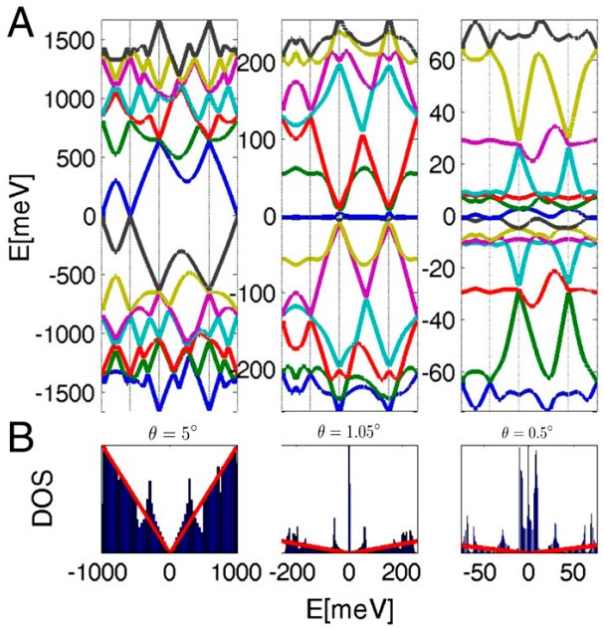

FIG. 9: (A) Energy dispersion of twisted bilayer graphene for the 14 bands closest to the Dirac point plotted along the k-space trajectory for $w_0 = w_1 = 110$ meV, and $\theta 5^o$ (Left), 1.05^o (Middle), and 0.5^o (Right). (B) DoS of moire bands.

We define $\mathbf{q}_1 = \Delta K = k_\theta(0, -1)$, and the vectors related by $2\pi/3$ rotations $\mathbf{q}_{2,3} = k_\theta(\pm\sqrt{3}/2, 1/2)$. Then we can write the tunneling matrix elements as

$$H_{UD} = w_0 U_0(\mathbf{r})\sigma^0 + w_1 U_{AB}\sigma^+ + w_1 U_{BA}\sigma^- \tag{86}$$

$$U_0(\mathbf{r}) = e^{-i\mathbf{q}_1\cdot\mathbf{r}} + e^{-i\mathbf{q}_2\cdot\mathbf{r}} + e^{-i\mathbf{q}_3\cdot\mathbf{r}} \tag{87}$$

$$U_{AB}(\mathbf{r}) = e^{-i\mathbf{q}_1\cdot\mathbf{r}} + e^{i2\pi/3}e^{-i\mathbf{q}_2\cdot\mathbf{r}} + e^{i4\pi/3}e^{-i\mathbf{q}_3\cdot\mathbf{r}} \tag{88}$$

$$U_{AB}(\mathbf{r}) = e^{-i\mathbf{q}_1\cdot\mathbf{r}} + e^{-i2\pi/3}e^{-i\mathbf{q}_2\cdot\mathbf{r}} + e^{-i4\pi/3}e^{-i\mathbf{q}_3\cdot\mathbf{r}} \tag{89}$$

Note, in the simplest approximation $w_0 = w_1 \sim 110$meV . However, later work showed that inter layer relaxation, relaxation followed by intra-layer relaxation reduce the ratio $\kappa = w_0/w_1$ from unity to $= 0.8$ and further 0.75.

It turns out that in the continuum model considered here, the interlayer term greatly modifies the band structure, or it renormalizes the Fermi velocity. As shown in Fig. 9, the band structure changes a lot by varying the twisted angle. At some specific angle, the Dirac point disappears, instead a nearly flat band appears. These twisted angles where the flat bands emerge are called *magic* angles. The flat bands are the origin of many interesting phenomena such as Mott insulator and superconductivity. (These concepts will be discussed

in a near future.) In 2018, Cao et al. (2018a) discovered an insulating behavior in twisted bilayer graphene at the magic angle 1.1^o, which is supposedly caused by many-body effects (Mott insulator). In the doped case, the system becomes superconducting (Cao et al., 2018b). Currently this is a subject of very intensive experimental and theoretical studies.

Nowadays, twist-angle adds a new degree of freedom to the band structure engineering, which increases the tunability of materials. Twisted materials have become a playground even for correlated physics, attracting much attention in physics.

HOMEWORK

1. Please analyze the crystal structure and orbital physics of a typical material that you are familiar with. You can choose any material, e.g. some materials under study in your group. If you donot have any idea, please try to analyze material 2D CuO_2 plane, which is the parent compound of cuprates.

2. Please calculate the density of states (DoS) of the single-layer graphene.

3. Is there any other symmetry (other than lattice inversion and time-reversal symmetry) of the single-layer graphene ? Please write down the analysis of invariance.

[1] Novoselov, K. S., Geim, A. K., Morozov, S. V., et al. (2004). Science 306, 666

[2] Katsnelson, M. I., Novoselov, K. S., Geim, A. K. (2006). Nature Phys. 2, 620

[3] Cheianov, V. V., Falko, V., Altshuler, B. L. (2007). Science 315, 1252

[4] Brey, L., Fertig, H. A. (2006). Phys. Rev. B 73, 235411

[5] Rafi Bistritzer and Allan H. MacDonald, PNAS 108, 12233–12237 (2011)

[6] Nature 556, pages 80–84 (2018); Nature volume 556, pages 43–50 (2018).